JOURNAL OF Materials CHEMISTRY

A Monte Carlo analysis of spin dynamics and Mössbauer relaxation in 3-D magnetically diluted iron oxides

Terence C. Gibb

School of Chemistry, The University, Leeds, UK LS2 9JT

Received 5th July 2000, Accepted 10th October 2000
First published as an Advance Article on the web 3rd January 2001

The spin dynamics of three-dimensional magnetically diluted iron oxides with the cubic perovskite structure have been studied by a Monte Carlo analysis using both the uniaxial Ising model and the isotropic Heisenberg model. The importance of a weak superexchange involving next nearest neighbours (nnn), in addition to the much stronger nearest neighbour (nn) superexchange, has been assessed. In the Ising case, below the critical temperature, antiferromagnetic domains are formed in which the domain walls are 'pinned' by the non-magnetic atoms such that increasing dilution causes substantial interpenetration of the domains, which is accentuated by nnn superexchange. Using the Heisenberg model, the vector nature of the spins prevents pinning, but a nnn superexchange of only 3–5% can cause spin rotation in localised clusters, and ultimately destroys the coherence of long-range order even though individual spins are still strongly coupled. The observed Mössbauer relaxation can be simulated for both models, and different relaxation rates are found for spins that have different numbers of nn and nnn spins. However, the observed spectra are apparently more consistent with Ising-like behaviour in the critical region, and it is suggested that local anisotropy may be an important factor in these diluted systems, which would traditionally be expected to behave as Heisenberg magnets.

Compounds with the stoichiometry ABX_3 and the cubic perovskite structure are regarded as ideal for the study of magnetic superexchange interactions.[1] The linear B–X–B nearest neighbour (nn) superexchange pathway is dominant and usually antiferromagnetic. The next nearest neighbour (nnn) superexchange pathway is usually assumed to be unimportant, and this may well be true in perovskite fluorides. Although many perovskites are distorted by tilting of the BX_6 polyhedra with B–X–B angles deviating from 180°, this does not appear to prevent the formation of an antiferromagnetic structure with long-range order. In perovskite oxides, the higher charges on the ions will introduce a significant degree of covalency, and evidence is emerging to suggest that this can result in the nnn superexchange becoming much more important. In particular, the discovery[2,3] of spin-glass behaviour in Sr_2FeNbO_6 and Sr_2FeRuO_6 strongly suggests that this is the case. The Fe and Nb or Ru cations are disordered,[3,4] while the Fe concentration on the B sites of $p = 50\%$ is well above the percolation limit of $p_c = 31.16\%$ so that antiferromagnetic order would be expected. Other compounds that have been found to behave analogously[5] are Ca_2FeNbO_6, Ba_2FeNbO_6, Ca_2FeTaO_6, and Sr_2FeTaO_6. In all cases the zero-field-cooled (ZFC) and field-cooled (FC) magnetic susceptibility data show hysteresis below *ca.* 25 K, while the ^{57}Fe Mössbauer spectra broaden below 30 K and ultimately develop a magnetic hyperfine spectrum at 4.2 K, suggesting that the Fe spins are 'freezing' at low temperatures. Neutron diffraction measurements on Sr_2FeRuO_6 and Sr_2FeTaO_6 at low temperature[3,6] show no evidence of long-range magnetic order.

On the other hand, $SrLaFeSnO_6$ which is also disordered on both A and B sites shows conventional antiferromagnetic order[7] below 250 K, with similar behaviour[8] observed in $BaLaFeSnO_6$ and $SrEuFeSnO_6$, although $CaLaFeSnO_6$ shows evidence of some cation ordering. However, the magnetic susceptibility in these compounds shows hysteresis between the ZFC and FC data below 250 K, as well as significant magnetic relaxation in the ^{57}Fe and ^{119}Sn Mössbauer spectra to well below 150 K. The magnetic moment, determined[7] by neutron diffraction at 1.7 K on $SrLaFeSnO_6$, was 2.94 μ_B, which is abnormally low.

Mössbauer relaxation is well known in magnetically diluted oxides including the ferrimagnetic spinels, and the existence of magnetic clusters is often assumed (following the work of Ishikawa[9]), which increase in size with decreasing temperature until long-range order is achieved. However, a convincing theoretical explanation for the behaviour of a diluted spin system as regards the Mössbauer relaxation has been lacking. Similar relaxation behaviour has been seen[10] in diluted oxides with the 'two-dimensional' K_2NiF_4 structure. In a recent paper[11] the dynamics of a 2-D Ising lattice as a model for magnetically diluted $SrLaFeO_4$ have been studied by a Monte Carlo analysis. The formation of antiferromagnetic domains, in which the domain walls (*anti*-phase boundaries) are pinned by the non-magnetic atoms, is seen to be an important factor in producing the magnetic hysteresis. Mössbauer relaxation can be simulated, and it is evident that spins with few nearest neighbour spins, particularly those close to a domain boundary, will relax faster. However, the old 'spin cluster' interpretation is not a good model.

In this paper, a Monte Carlo analysis of a 3-D magnetically diluted cubic perovskite lattice is described using both the uniaxial Ising and the isotropic Heisenberg models for the magnetism. The calculations described are mainly linked to a magnetic concentration of $p = 50\%$ to enable comparison with the experimental data that are available.

The simulation methods

In the diluted K_2NiF_4 structure the magnetism is very close to ideal 2-D planar, and the spin ½ 2-D Ising model was used[11] to simulate the magnetic behaviour. Although the computational model adopted only two spin states for each ion represented by $+1$ and -1, which will not describe the $S = 5/2$ Fe^{3+} ion accurately, the basic approach succeeded in reproducing the

 DOI: 10.1039/b005383j

observed phenomena. The same 2-D Ising model for the magnetisation has been evaluated for the 3-D spin system, because it was thought to be helpful to compare the extremes of the Ising and Heisenberg models.

The linear Fe–O–Fe nn superexchange is represented by $Js_i^z.s_j^z$ where J is the superexchange coupling constant. There are 24 Fe–O–B–O–Fe superexchange pathways to the 12 nnn B sites which can be represented in terms of J_2. Two limiting cases were considered. In Model 1, all 24 superexchange pathways were considered to be equivalent regardless of the nature of atom B. In Model 2, only those pathways in which B was not Fe were considered. The thermal temperature was represented in reduced units as kT/J, and an applied magnetic field B could be included. In this way the energy of each spin in the Ising model can be written as

$$E_i = -s_i\left(J\sum_1^6 s_j + J_2\sum_1^{24} s_k\right) - Bs_i$$

The computer code for the simulations was written in the C language. An N^3 matrix of spins was created at random with a concentration of magnetic spins of $0 \leqslant p \leqslant 100\%$. The spin system was then allowed to evolve using Monte Carlo methods as previously described,[11] using periodic boundary conditions to remove the edge effects. One Monte Carlo step (MCS) corresponds to N^3 random attempts at spin reversal. Data sets of 50^3 and 100^3 atoms were used, and a typical cooling cycle used n MCS at $kT/J = 3.0$, repeating at decrements of 0.1 until $kT/J = 0.1$. Typically $n = 2000$ MCS with 1000 MCS to establish near equilibrium and 1000 MCS for data collection. The largest in-phase and out-of-phase antiferromagnetic percolation clusters were determined,[11] together with statistical information on the domain boundaries. Various sizes of data set, and different random site occupation and starting points were used, and the features described here (for both Ising and Heisenberg models) are considered to be effectively independent of these parameters. However, only representative calculations will be discussed in this paper.

The 3-D Heisenberg model can be expected to give a better representation of the isotropic Fe^{3+} (d^5) spin system. The main difference is that each spin is represented as a unit vector in space using s_x, s_y and s_z as component vectors. For a cooling cycle these vectors are generated to give random orientations of the spins. The magnetic field was applied along the z direction. The energy of spin i can be written as

$$E_i = -J\sum_{j=1}^{6}\left(s_{ix}s_{jx} + s_{iy}s_{jy} + s_{iz}s_{jz}\right)$$
$$-J_2\sum_{k=1}^{24}\left(s_{ix}s_{kx} + s_{iy}s_{ky} + s_{iz}s_{kz}\right) - Bs_{iz}$$

Data sets of 20^3 and 40^3 atoms including periodic boundary conditions were used. At each attempt at spin reversal, a prospective new spin vector was calculated: the three spin vectors were allowed to change randomly by a small increment up to a pre-set limit, and renormalized to a unit spin vector. A decision was then made to accept the new spin vector, or retain the original vector, by using the familiar Metropolis method. The spin system inevitably evolves more slowly than in the Ising calculation, and a cycle of 10 000 + 10 000 MCS was adopted at each temperature. This necessarily limits the size of the spin system which can be used, but produces better estimates of the averages over all spins for $\langle S_x\rangle$, $\langle S_y\rangle$ and $\langle S_z\rangle$ and the average spin value $\langle S\rangle$.

The final values of the three spin vectors (in the range $-1 < 0 < +1$) were converted to integers in the range 0–200. These were used as red–green–blue values for a coloured graphical display of the spin system with the staggered correlation of the antiferromagnetic order included. The model does not include the simple *anti*-phase boundaries of the Ising model because the spins are vectors. However, as shown by the examples included here, the colour display can reveal clearly groups of spins with different orientations, and therefore gives an indication of the overall coherence of the spin system.

Models for nnn interactions

A major objective is to understand why for example $SrLaFeSnO_6$ is an antiferromagnet (albeit with a reduced Fe moment), whereas Sr_2FeNbO_6 and Sr_2FeTaO_6 show no ordered moment. All of these compounds show cation disorder. The high-spin Fe^{3+} cation can be relied upon to give strong superexchange interactions in a perovskite, and in $LaFeO_3$ where the tilting of the FeO_6 octahedra reduces the bond angle to 157°, the Néel temperature is still a respectable 740 K. The most likely cause of spin frustration is competition between the nn and nnn superexchange interactions, which would both have to be antiferromagnetic. Nevertheless, this is clearly ineffective in $LaFeO_3$ even though the ratio of J_2/J may be non-zero. The covalent overlap of Fe^{3+} with O^{2-} will be much stronger than the equivalent behaviour in a perovskite fluoride where the charges are smaller. When the non-magnetic B cation has a nominal charge of +3 (Fe) or +4 (Sn) then the compound is an antiferromagnet, but if the charge is +5 (Nb or Ta) then the long-range order is lost.

It is reasonable to postulate that the nnn superexchange is strong enough to cause the frustration of those spins having only a small number of nn spins. Moreover, the increased covalency associated with a higher charge on the intermediate cation should increase the nnn superexchange. Model 1 in which all 24 nnn superexchange pathways are assumed to be equivalent is representative of $LaFeO_3$ and perhaps $SrLaFeSnO_6$, whereas Model 2 with nnn superexchange *via* the non-magnetic cation only is a more extreme view which can be applied to Sr_2FeNbO_6 and Sr_2FeTaO_6. The true situation may be intermediate. The new results for Monte Carlo simulations with $p = 50\%$ and for various values of J_2/J throw additional light onto the problem.

Quenched 3-D Ising and Heisenberg spin systems

Various aspects of the behaviour of 3-D Ising spin systems have been described previously by Nowak and Usadel in a series of studies[12–17] of models for a diluted Ising antiferromagnet in a magnetic field (DAFF), and for a random field Ising ferromagnet (RFIM). These papers only consider the nn superexchange interaction, but nevertheless provide useful support for the present study.

As with the earlier study[11] on 2-D spin systems, the dynamic evolution of a 3-D Ising spin matrix quenched (instantaneously) from high temperature provides a useful insight into the dynamic approach to the equilibrium state. This procedure is of course artificial, and realistic rate information cannot be obtained, but nevertheless it does help to understand this very complex problem of diluted spin systems. A matrix of 100^3 atoms with $p = 50\%$ was created in a random state, instantaneously cooled to $kT/J = 0.5$ (a reduced temperature of $T/T_N \approx 0.25$, where T_N is the Néel temperature, and therefore still with significant thermal energy) and allowed to relax towards equilibrium in the absence of a magnetic field. The spin system was then examined at appropriate intervals, and the largest in-phase and out-of-phase antiferromagnetic percolation clusters examined as described for the 2-D systems.[11]

After only 50 MCS some 44% of the spins are in the reversed direction, but 96% of the spins are now incorporated into two

large interpenetrating domains of effectively equal size. Such domains have been described previously[14] and are considered to be essentially fractal in nature. It is logical to expect initially that small in-phase and out-of-phase domains will form at random, but the intergrowth of very large domains is somewhat of a surprise, and does not appear to be size limited as the same effect is seen in matrices of differing size. From this stage onwards the rate of flipping decreases slowly, but more importantly the number of atoms that have changed at the end of a period of say 2000 MCS is quite small. In fact a significant number of the flips will be due to magnetically isolated spins (1.6%) that can flip repeatedly with a probability of 50%.

It is fortuitous that the concentration of interest ($p=50\%$) corresponds to the marked development of interpenetrating domains. The important factor is undoubtedly the 'pinning' of the domain walls by the non-magnetic atoms. The number of atoms in a domain wall decreases slowly, and after 10 000 MCS only 6% of these have more than 1 *anti*-phase neighbour. A typical spin matrix after 10 000 MCS is shown in Fig. 1. It is not easy to illustrate the 3-D assembly of spins, and the in-phase and out-of-phase antiferromagnetic spins are shown in black and grey respectively, with non-magnetic atoms in white. Only the faces of the cube can be seen. The domains remain highly intergrown, reach all six faces of the cube, and contain over 96% the spins. Visual representation of the spins at 50 and 10 000 MCS differ in the fine detail rather than in any dramatic local consolidation of domain structure. The 3-D staggered correlation function can be represented by

$$c(r)=\left\langle \frac{1}{2n^2}\sum_{i=1}^{n}\sum_{j=1}^{n}(-1)^r\left(s_{ij,\frac{n}{2}}s_{ij,\frac{n}{2}+r}+s_{ij,\frac{n}{2}}s_{ij,\frac{n}{2}-r}\right)\right\rangle$$

as the correlation of pairs of spins s_{ijk} at $\pm r$ cell spacings on either side of a reference plane of n^2 spins at $k=n/2$. A plot of $\ln[c(r)]$ against r has a slope of $-1/\lambda$ where λ is the correlation length. However, λ should be viewed as a measure of interpenetration rather than as an indication of domain size. The value of λ increases slowly from 1.6 to 4.6 cell spacings for 50 and 10 000 MCS respectively, and demonstrates that the approach to a fully ordered state is exceedingly slow.

These data illustrate that the Ising 3-D spin system with $p=50\%$ shows domain pinning in the same way as described earlier for the Ising 2-D spin system. In fact the very small correlation length would preclude the observation of antiferromagnetic long-range order by neutron diffraction, and the system is therefore best described as a spin-glass in nature. The intergrowth structure observed is also dependent on the sampling method, so that effectively the system appears to have a multiple ground state, another characteristic of a spin-glass. On the other hand a magnetically concentrated ($p=100\%$) spin system under the same conditions evolves rapidly towards a single-domain structure within 1000 MCS.

Similar calculations for quenching of a 3-D Heisenberg system were carried out using a random matrix of 40^3 atoms with nn interactions only and a concentration of $p=50\%$. The temperature was instantaneously reduced to $kT/J=0.1$, corresponding to a reduced temperature T/T_N of *ca.* 0.2 to allow some residual thermal energy. The system rapidly adopted a single-domain structure, appearing to reach an equilibrium state within 20 000 MCS. The average value of S taken over all the spins was $\langle S\rangle=0.883$. There is thus a marked difference between the anisotropic Ising model that develops an interpenetrating domain structure by 'pinning', and the isotropic Heisenberg model where the free rotation of the spin vector prevents such an effect.

Slowly-cooled 3-D Ising spin systems

The same random spin matrix develops very differently in a slow-cooling regime from $kT/J=3.0$ to 0.1 in decrements of 0.1 with 1000 + 1000 MCS at each temperature. The development of long-range order in the vicinity of the critical temperature is difficult to monitor from a small number of simulations of finite size. A useful criterion appears to be to observe the number of spins that have changed orientation after 1000 MCS. If spins are flipping randomly, then 50% of the spins are reversed after this time interval. As long-range order appears on cooling, this fraction decreases rapidly towards zero as

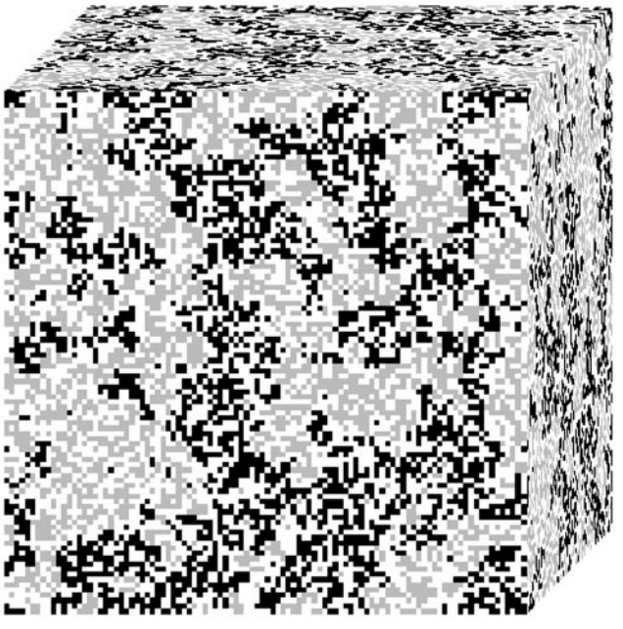

Fig. 1 The domain structure for a random Ising 3-D matrix of 100^3 atoms (with $p=50\%$, quenched to $kT/J=0.5$ and allowed to evolve for 10 000 MCS, as described in the text). Non-magnetic atoms are shown in white, while in-phase and out-of-phase antiferromagnetic domains are shown in black and grey respectively. Close inspection of the data shows the existence of large numbers of non-magnetic atoms along the domain boundaries. Over 97% of the spins belong to the two largest intergrown percolation clusters.

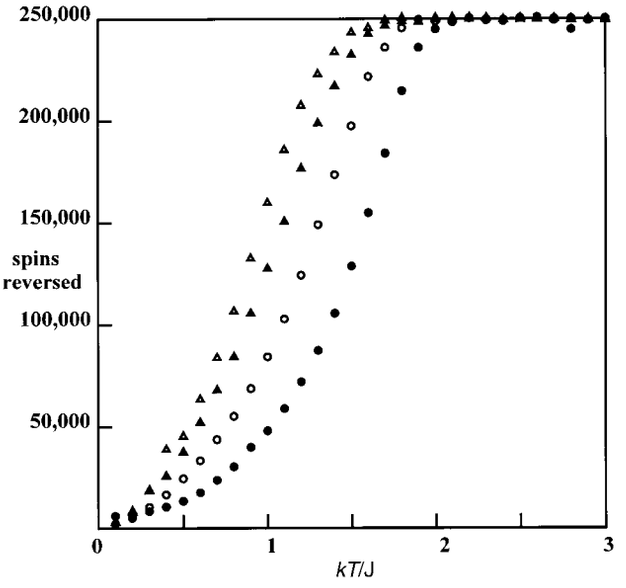

Fig. 2 The number of spins in a 100^3 matrix of atoms with $p=50\%$ that reverse direction after 1000 MCS as a function of temperature. At high temperature where the flipping is rapid 50% of the spins (250 000) will reverse direction. As spin alignment begins to take place below T_N the number of reversed spins drops rapidly. With increasing values of J_2/J (0 filled circles, 0.05 open circles, 0.10 filled triangles, 0.15 open triangles) the ordering temperature decreases and becomes more diffuse.

illustrated in Fig. 2. The filled circles correspond to $J_2=0$ (the other data are described later). This criterion was applied[11] to the 2-D Ising systems, and is also useful in the present instance. It is not clear as to whether the first signs of slowing of the spins are due to order over long ranges, or rather to the development of large fractal clusters which may still be dynamic, but are nevertheless relaxing very slowly. Certainly percolating clusters that are dynamic are often seen just above the critical temperature, and indeed for $p>62.4\%$ this will always be true.

The following observations were made for a typical calculation. The critical temperature for $J_2=0$ (*i.e.* for nn interactions only) is at approximately $kT/J=2.0$. Spins with no nn spins flip rapidly at all temperatures. Spins with 1 and 2 nn spins are flipping rapidly for $T/T_N>0.25$ and 0.5 respectively. The energy of the system approaches the equilibrium value within the first 500 MCS. The matrix at $kT/J=0.1$ is shown in Fig. 3. The two largest domains contain almost the same numbers of spins, and together this amounts to 97.9% of the total. Some isolated spins are evident, and the domain boundaries are associated with large numbers of non-magnetic atoms. The number of spins with 2 (or more) out-of-phase nn interactions decreases rapidly below the critical temperature, although some 1% of spins retain one nn contact, and can be considered as being in a domain wall. The final domain structure is already clearly evident at $kT/J=1.5$, after which the domain walls only consolidate at lower temperatures without any major movement. However, the final domain structure is dependent on the random nature of the spin flips, and seeding the random number generator with a different starting point will produce a visibly different end result of almost the same energy. Thus the model can be regarded as having a degenerate energy state. The energy calculated is within 2% of that for the ideal single-domain lattice, but this ideal state may never be achieved because the spins are 'pinned' by the domain walls. A similar calculation in reverse, starting from the fully ordered state and then raising the temperature, produces large *anti*-phase clusters only for $kT/J>1.8$, but the energy and the numbers of spin flips are very similar with only a comparatively small degree of hysteresis.

If J_2 is allowed to become non-zero to all next nearest neighbours (Model 1), then spins with a large nnn/nn occupation ratio will tend to be reversed. This results in a much lower energy than might have been the case, and also increases the interpenetration of the domains, as seen in Fig. 4 for $J_2=0.1$. Indeed, the energy achieved on cooling is *below* that calculated for the ideal ordered state, and is clearly an important factor in controlling the domain system. However, in this example there are still two domains containing 95.0% of the spins, but the number of atoms in the domain walls is now 23%. The number of spins flipped after 1000 MCS for $J_2=0$, 0.05, 0.10, and 0.15 are plotted in Fig. 2. It can be seen that the increasing nnn interaction effectively decreases the transition temperature, and the transition itself is more diffuse.

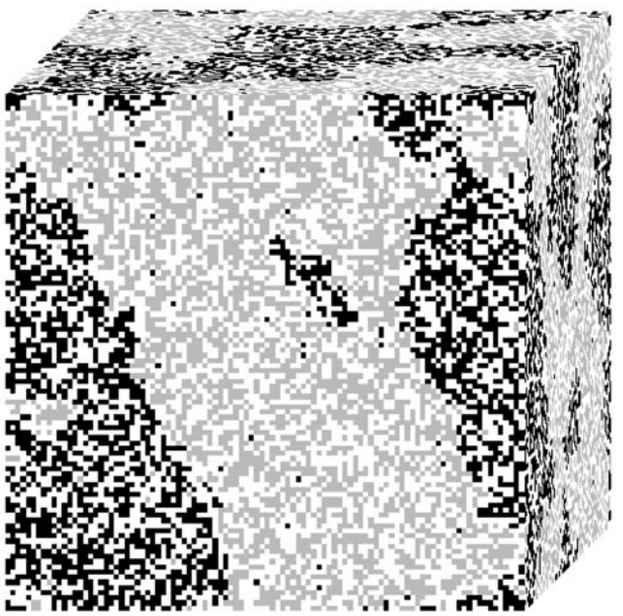

Fig. 3 The domain structure for the Ising 3-D matrix shown in Fig. 1, after slowly cooling from $kT/J=3.0$ to 0.1 with $1000+1000$ MCS per step, as described in the text. The two largest intergrown percolation clusters contain 97.9% of the spins, but the intergrowth is less, and the correlation length is now 9.4 cell spacings.

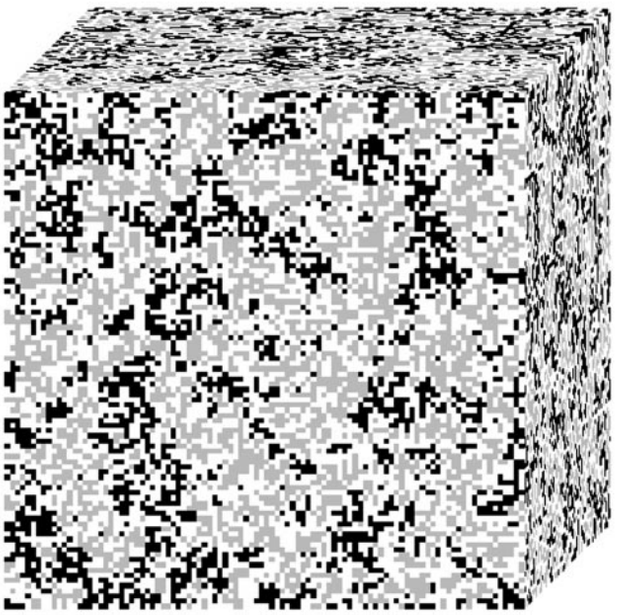

Fig. 4 The domain structure for the Ising 3-D matrix shown in Fig. 3, after the same cooling process from $kT/J=3.0$ to 0.1 with $1000+1000$ MCS per step, but with a non-zero nnn interaction of $J_2/J=0.10$. The two largest percolation clusters are more intergrown, and the correlation length has decreased to 6.4 cell spacings. The energy is actually lower than would be the case for perfect antiferromagnetic alignment, and illustrates how the domain formation is partially energy driven.

Slowly cooled 3-D Heisenberg spin systems

The undiluted ($p=100\%$) simple cubic Heisenberg lattice with antiferromagnetic nn (J) and nnn (J_2) interactions is of interest[18] because of the potential for frustration. When J_2 is small, then the energy (for *anti*-parallel nn spins) can be written as $E=\sum(-6J+24J_2)$. Spin frustration can occur for $J_2/J=0.125$. For $J_2/J>0.125$ the ground state is one of three equivalent collinear configurations in which adjacent planes of antiferromagnetic spins are coupled ferromagnetically. These three situations were realised in some test runs of the Heisenberg Monte Carlo calculation that gave a useful verification of the methodology. A random spin system with $p=100\%$ was equilibrated for a particular value of J_2 at $kT/J=3.0$ for $1000+1000$ (or $10\,000+10\,000$) MCS, and cooled to $kT/J=0.1$ in decrements of 0.1. The different spin arrangements described above were observed. However, in the present context an increasing magnetic dilution will eventually have a dramatic influence on the spin system, and one would expect significant frustration to develop locally in the lattice for values of J_2/J deviating substantially from 0.125.

Much more detailed simulations were carried out for 20^3 and 40^3 atoms at $p=50\%$ with equilibration at $kT/J=0.80$ for $1000+1000$ (or $10\,000+10\,000$) MCS, and cooled to $kT/J=0.025$ in decrements of 0.025 (note that the Ising and

Heisenberg calculations are not scaled identically). The values of the spin vectors were not averaged close to zero during 1000 MCS above the critical temperature, but 10 000 MCS proved satisfactory in this regard. The final data reported here were all obtained for 40^3 atoms and 10 000 MCS to establish equilibrium, and a further 10 000 MCS to obtain data values. Each calculation took several days to run. It is believed that these figures give a reasonable representation of the isotropic Heisenberg spin system, and that the influence of the size of the data set and the number of MCS has been adequately considered.

The energy of a matrix of 20^3 atoms as a function of J_2/J is shown in Fig. 5, together with the value of $\langle S \rangle$ after a slow-cooling cycle with 10 000 + 10 000 MCS per decrement. Both Model 1 and Model 2 are represented. Also included are the values of the energy for a perfectly aligned antiferromagnetic state. The (negative) energy from the spin interactions initially decreases almost uniformly with increasing J_2/J, but by $J_2/J = 0.04$ a significantly larger magnetic energy can be gained by allowing spin misalignment. At the same time, the value of $\langle S \rangle$ as a measure of ordered spin alignment decreases rapidly to *ca.* 0.5 at $J_2/J = 0.04$ (a nnn exchange of only 4%). Model 2, in which only the exchange *via* the diamagnetic atoms is considered, is only marginally less effective in destroying long-range order. This is compatible with spin misalignment being more likely when the number of nn neighbours is smaller.

Another way of following the effect of J_2 on the ordering is to consider the value of $\langle S \rangle$ as a function of both J_2/J and kT/J as shown in Fig. 6. The data shown are for 40^3 atoms and 10 000 + 10 000 MCS per decrement using Model 2, but very

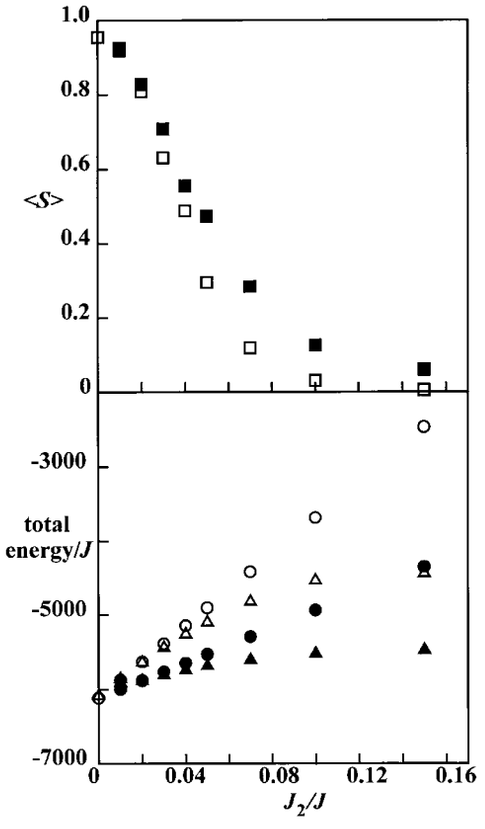

Fig. 5 The lower diagram shows the final energy of a matrix of 20^3 atoms as a function of J_2/J after a slow-cooling cycle with 10 000 + 10 000 MCS per decrement (triangles), while the upper diagram similarly shows the value of $\langle S \rangle$ (squares). Data for Model 1 and Model 2 are represented as open and filled symbols respectively. The circles represent the values of the energy for a perfectly aligned antiferromagnetic state, showing that spin misalignment lowers the energy when J_2/J is non-zero. The value of $\langle S \rangle$ as a measure of ordered spin alignment decreases rapidly with increase in J_2/J.

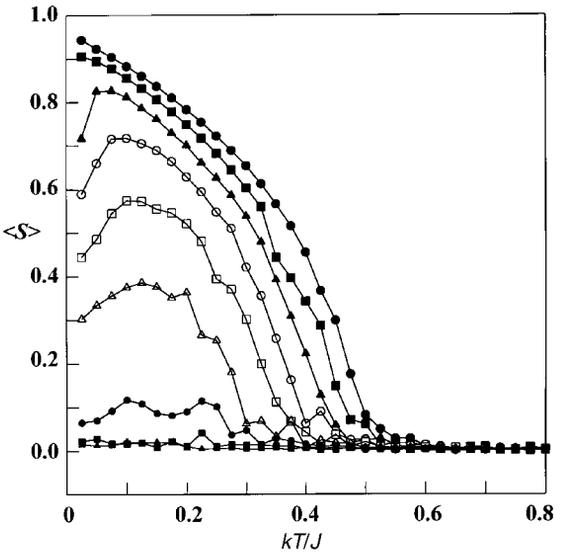

Fig. 6 The value of $\langle S \rangle$ as a function of both J_2/J and kT/J for 40^3 atoms and 10 000 + 10 000 MCS per decrement using Model 2. The values of J_2 from top to bottom are 0.00, 0.01, 0.02, 0.03, 0.04, 0.05, 0.07, 0.10, and 0.15. An increase in J_2/J causes a decrease in T/T_N and a rapid decrease in $\langle S \rangle$. The conclusion can be drawn that the nnn antiferromagnetic interactions can result in a significant reduction in the observed magnetic moment as defined by $\langle S \rangle$, and could effectively destroy the long-range order from a neutron diffraction stand point.

similar results are seen for smaller data sets. An increase in J_2/J causes a decrease in T/T_N ($\sim$0.20 for $J_2/J = 0.03$) and a rapid decrease in $\langle S \rangle$ for $0.3 < J_2/J < 0.7$. An unexpected feature of the latter is a marked decrease in $\langle S \rangle$ for $kT/J < 0.1$. However, it seems plausible that the smaller J_2 value can be responsible for a progressive local spin rotation at the lower temperatures as the thermal energy is removed. Evidence for this is shown below. The conclusion can be drawn that the nnn antiferromagnetic interactions can result in a significant reduction in the observed magnetic moment as defined by $\langle S \rangle$. Thus the moment of 2.94 μ_B in $SrLaFeSnO_6$ could mean a J_2/J ratio of only about 3%, whereas an increase to 6% for Nb and Ta would effectively destroy the long-range order from a neutron diffraction stand point.

It is not a trivial matter to understand the microscopic nature of the spin alignment in three dimensions. A further visualisation of the way in which the long-range order is destroyed despite the presence of strong nn spin interactions can be obtained by representing the spin direction as coloured squares using red, green, and blue components to mimic the three orthogonal directions which comprise the individual spin vector. Fig. 7 shows typical data for a 40^3 matrix after slowly cooling to $kT/J = 0.025$ with 10 000 MCS per decrement, and with J_2/J values of 0.00, 0.03, 0.05 and 0.10. When $J_2/J = 0$ the spins align essentially parallel to each other as shown by the uniform colour, with the exception of isolated spins which are not coupled to the rest of the matrix. It is clearly evident that comparatively small values of J_2/J can result in small clusters of spins, largely segregated from the bulk by non-magnetic atoms, that differ markedly in orientation from adjacent clusters as shown by the changes in colour, while a substantial spin rotation can occur within regions of poor contact. Thus percolation alone is no longer a sufficient condition to cause spin alignment, and in this respect the isotropic Heisenberg model differs very significantly from the anisotropic Ising model.

Spin relaxation in an applied magnetic field

The magnetically diluted perovskites should show ideally no difference between the magnetism observed (a) when the spins

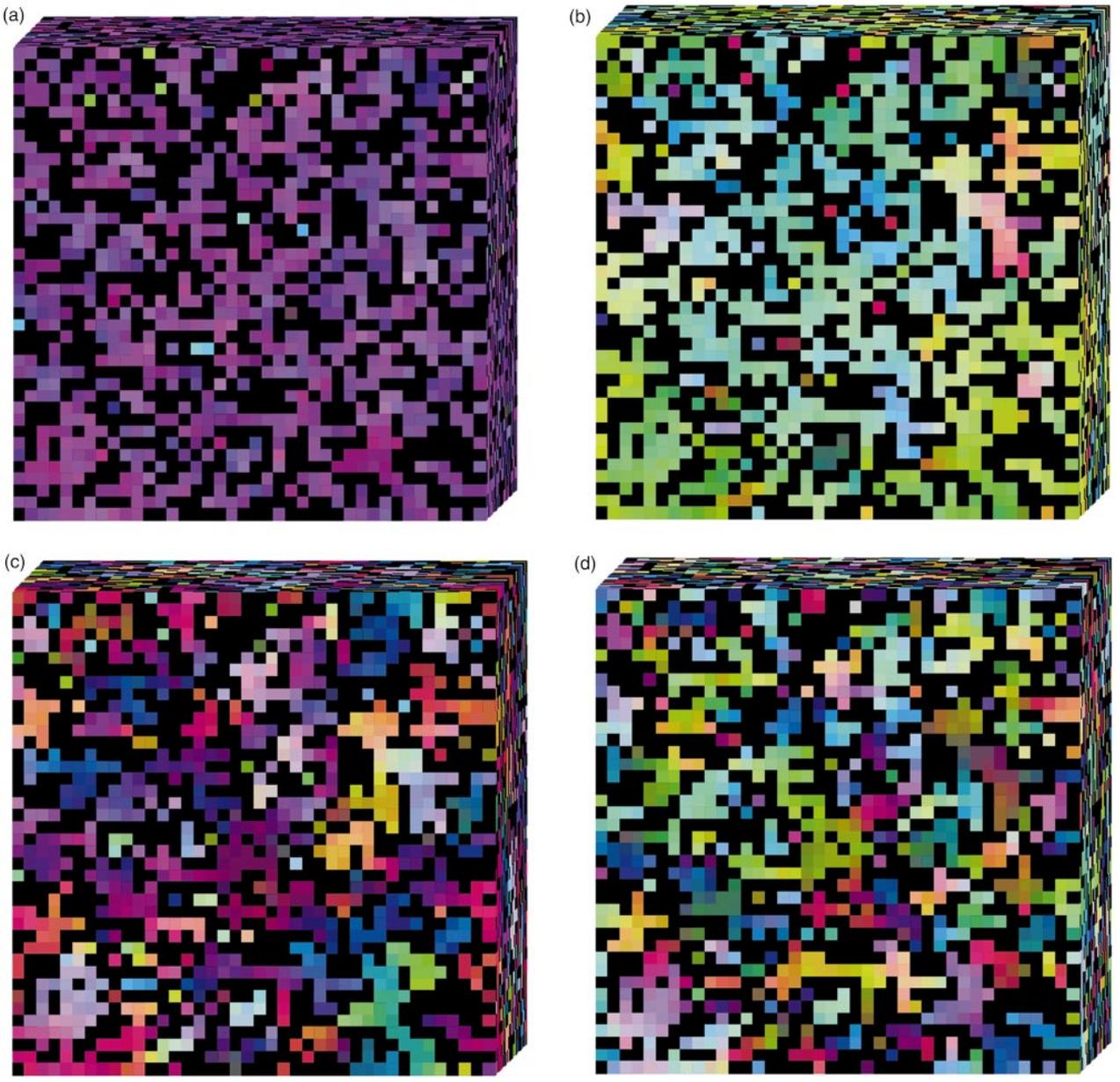

Fig. 7 A representation of a 40^3 matrix of atoms after cooling to $kT/J=0.025$ with 10 000 MCS per decrement for J_2/J values of (a) 0.00, (b) 0.03, (c) 0.05, and (d) 0.10. The non-magnetic atoms are shown in black, while the spin orientation is represented by a colour with the red–green–blue intensities scaled to the corresponding x, y, z spin vectors. Increasing values of J_2/J cause increasing spin misalignment and small regions of nearly parallel spins separated by largely non-magnetic boundaries.

are slowly cooled through the critical temperature *before* a field is applied and the magnetism recorded during heating (a ZFC experiment), and (b) when the field is applied and the spins are slowly cooled through the critical temperature while the magnetism is recorded (a FC experiment). However, experimental data[2,5,7,8] have revealed a pronounced hysteresis in the magnetic behaviour suggestive of a multiple ground state. In the 2-D magnetically diluted oxide systems it was shown[11] that this could occur in an Ising lattice by the interpenetration and pinning of the domain walls.

Calculations for a 3-D Ising lattice confirm that similar behaviour can be predicted. Simulations were made for 100^3 atoms using 1000+1000 MCS at each temperature step as described earlier, but with the appropriate application of an applied field $H/J=1$ or 0.1. A large value of the field is necessary because of the finite size of the simulation. Some typical data sets are shown in Fig. 8. The field that is applied along the unique axis causes an imbalance in the number of spins parallel and antiparallel to the field. And the fractional imbalance can be crudely related to the effective magnetisation M. Hysteresis is shown in Fig. 8 for $J_2/J=0$ and 0.05 with $H/J=1$, and for $J_2/J=0.05$ and $H/J=0.1$, and indeed is a feature

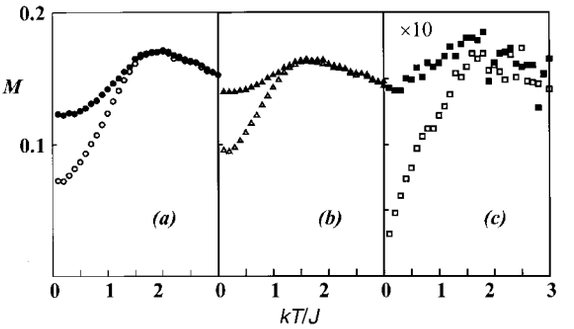

Fig. 8 The magnetisation M of an Ising matrix of 100^3 atoms with 1000+1000 MCS per increment as a function of kT/J for the values (a) $J_2/J=0.00$ and $H/J=1$, (b) $J_2/J=0.05$ and $H/J=1$, (c) $J_2/J=0.05$ and $H/J=0.1$. In all cases there is a distinct hysteresis between the ZFC (open symbols) and FC (filled symbols) calculations.

of all simulations carried out for a wide range of J_2/J and H/J values. As J_2/J increases the interpenetration of the domains also increases markedly.

A number of FC and ZFC simulations for both Model 1 and Model 2 with a 20^3 Heisenberg lattice, an applied field of $H/J=1$, and for various values of J_2/J showed no significant evidence for magnetic hysteresis. This is in sharp contrast to the pronounced hysteresis found using the Ising model, but is not too surprising as the isotropic spin rotation of the Heisenberg system precludes the pinning of spins at low temperatures. This does lead, however, to a belief that the experimental observations of hysteresis must reflect a degree of anisotropic behaviour in the spin system. A likely cause of this is the local distortions caused by randomly placed ions of differing size and charge, although no attempt has been made to include these effects in the present calculations.

Relaxation in Mössbauer spectra

In an attempt to demonstrate the effect of the spin dynamics on relaxation of the Mössbauer spectrum, the calculations described above included the calculation of a histogram of the $\langle S_i \rangle$ values from 0 to 1 in units of 0.01. A series of 100 Mössbauer spectra using the same increments and a maximum flux density of 50 T were calculated, and then summed with weightings from the histogram.

A 3-D Ising simulation for Model 1 using 100^3 atoms and $1000+1000$ MCS, given in Fig. 9, shows the development with decreasing temperature of broad magnetic wings beneath a collapsed central feature, very similar to experimental observations for $SrLaFeSnO_6$. Even for $J_2/J=0$, the central feature is apparent at $kT/J=1.5$ (T/T_N *ca.* 0.75). A similar series of calculations for $J_2/J=0.10$ differ principally in that the equivalent spectra are now at a reduced temperature some 0.5 lower than before. The spin system still 'freezes', but at a significantly lower temperature.

Simulations using the Heisenberg lattice with Model 2 required 10 000 MCS to prevent unrealistic line broadening above T_N because of inadequate averaging of the spins. For $J_2/J=0$, the characteristic 6-line pattern develops quite quickly below T_N as illustrated in Fig. 10. For $J_2/J=0.05$, the initial broadening below T_N retains a central collapsed component at much lower reduced temperatures as shown in Fig. 11, and significant line broadening is still present at temperatures far below the critical temperature. Thus in a Heisenberg spin system the introduction of nnn superexchange has a major effect on the relaxation behaviour. However, the Heisenberg simulations do not produce the central component on a broad background as seen in the Ising simulations and the experimental data. This lends further support to the suggestion that an isotropic model is not entirely appropriate. There is some direct evidence in that the local anisotropy at each site is known to result in a significant quadrupole splitting in the Mössbauer spectrum at room temperature.

The ^{119}Sn resonance in $SrLaFeSnO_6$ shows large transferred hyperfine fields but with considerable line broadening[7,8] even at very low temperatures, and there is a relaxational collapse as the temperature is raised. The existence of spin misalignment for $J_2>0$ is relevant to understanding the absence of resolved fine structure, and additional work is required on this aspect.

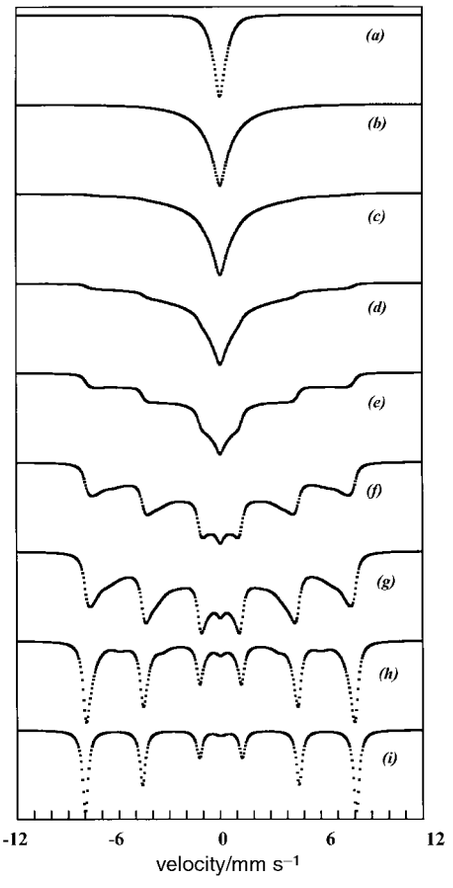

Fig. 9 A 3-D Ising simulation of Mössbauer relaxation using Model 1 for 100^3 atoms and $1000+1000$ MCS, showing the development with decreasing temperature of broad magnetic wings beneath a collapsed central feature, very similar to experimental observations for $SrLaFeSnO_6$. The vertical absorption scale is arbitrary for visual effect. The reduced temperatures, kT/J, correspond to values of (a) 3.0, (b) 2.0, (c) 1.9, (d) 1.8, (e) 1.7, (f) 1.6, (g) 1.5, (h) 1.0, and (i) 0.1.

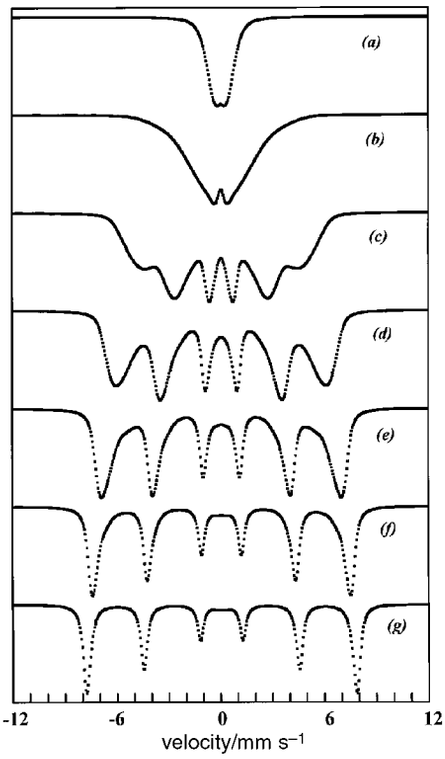

Fig. 10 A 3-D Heisenberg simulation of Mössbauer relaxation using Model 2 for 40^3 atoms and $10\,000+10\,000$ MCS, with $J_2/J=0$, showing the development with decreasing temperature of a broadened magnetic spectrum which persists over a considerable temperature range. The reduced temperatures, kT/J, correspond to values of (a) 0.8, (b) 0.5, (c) 0.4, (d) 0.3, (e) 0.2, (f) 0.1, (g) 0.025.

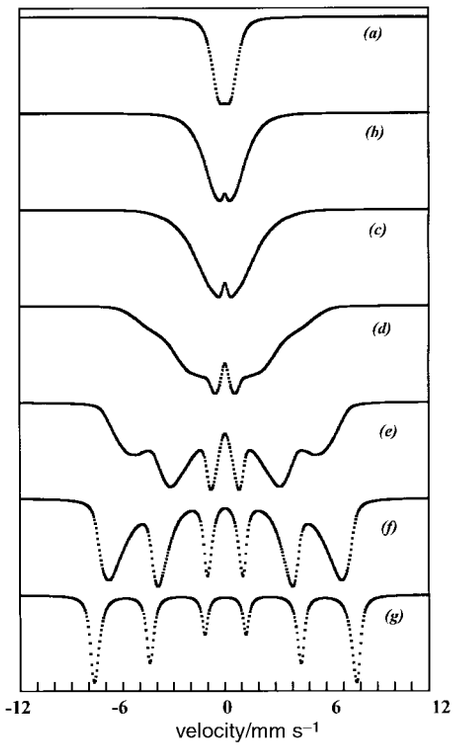

Fig. 11 A 3-D Heisenberg simulation of Mössbauer relaxation using Model 2 for 40^3 atoms and 10 000 + 10 000 MCS, with $J_2/J = 0.05$, showing the development of a broadened magnetic spectrum which persists over a more prolonged temperature range than for similar calculations in Fig. 10. The reduced temperatures, kT/J, correspond to values of (a) 0.8, (b) 0.5, (c) 0.4, (d) 0.3, (e) 0.2, (f) 0.1, (g) 0.025.

Discussion of the relevance of the model

The simulations described here still represent approximations to the real situation. In particular only one more distant superexchange is considered, and no account is taken of local lattice distortions. However, even these simple models have led to an improved understanding of the real systems. From an examination of the experimental data and the Monte Carlo simulations, it is suggested that the nnn spin interactions are more important when the intermediate cation has a high charge.

Useful evidence to support this belief is provided by Mössbauer spectroscopy, which can give direct information on induced spin densities at the intermediate cation, particularly for Sn and Sb. The spinel system $(Ni_yFe_{1-y})[Ni_{1-y+2x}Fe_{1+y-3x}Sb_x]O_4$ has been studied by observing[19] the super-transferred hyperfine interactions at diamagnetic ^{121}Sb ions. The metal oxidation states are Ni^{2+}, Fe^{3+}, and Sb^{5+}. An Sb atom on an octahedral B-site has 6 tetrahedral A-site neighbours. The ^{121}Sb Mössbauer spectrum for $x = 0.05$ (and with y close to zero) essentially shows a single magnetic flux density of 31.5 ± 1.0 T (despite the fact that the B-site neighbours are Fe and Ni at random). This clearly demonstrates that the B–B interactions are insignificant, and that the $\sim 125^\circ$ Fe–O–Sb transferred hyperfine interaction is about 5.3 T. Similar ^{119}Sn Mössbauer data[20,21] for $(Fe)[Ni_{1.125}Fe_{0.75}Sn_{0.125}]O_4$ show a maximum flux density of 25.0 ± 0.5 T (both values measured at around 80 K). In the former case the development of multiple ^{121}Sb fields with increasing x was attributed to an increase in Ni concentration on the A sites. In the latter, the multiple ^{119}Sn fields were originally linked to nn B-site populations, implying that B–B interactions are important, but in retrospect an A-site occupancy of $\sim 18\%$ Ni would almost certainly give a better analysis of the data. The similarity of the compositions of the two systems, coupled with the analysis described above, would suggest that the reinterpretation is valid.

A detailed theoretical analysis[22] of the possible spin transfer mechanisms for Fe–O–Sb has been made. The dominant interaction is a covalent overlap of $3d^5$ with the oxygen ligand orbitals, giving a transferred spin density on the ligand, which is similarly transferred through the Sb–O bond to the 5s orbital of Sb^{5+}. The mechanism for Fe–O–Sn transfer is the same (the ions are isoelectronic). A crude estimate of electron configuration gives $5s^{0.16}$ for Sb and $5s^{0.10}$ for Sn, and the transferred hyperfine fields are predicted to be in the ratio $H_{Sb}/H_{Sn} = 1.3$, which is broadly in agreement with observation[23] which suggests a figure of 1.25. The indications are that spin transfer mechanisms *via* Sb^{5+} are more effective than *via* Sn^{4+}, and are very much larger than Fe^{3+}–O–Fe^{3+} transfer. The argument may differ in detail for Nb^{5+} and Ta^{5+} because of the availability of empty d orbitals, but the importance of covalent overlap for nominally highly-charged ions must still be relevant. It seems reasonable to assume that a significant nnn antiferromagnetic coupling originates in this way, and that Model 2 for Heisenberg spin interactions is plausible. A more rigorous analysis is beyond the scope of this paper.

Finally, it is interesting to note that the super-transferred hyperfine fields at ^{119}Sn from 6 Fe neighbours in $LaFeO_3$, $EuFeO_3$, and $LuFeO_3$ doped with $CaSnO_3$ (with Fe–O–Sn bond angles of 157, 148, and 144.5° respectively) correspond to flux densities of 25.2, 19.6 and 15.8 T. Clearly the flux density decreases substantially with a decrease in bond angle.[24] However, the values for the spinels referred to above feature a transfer from a more covalent tetrahedral site with short Fe–O distances, while in the perovskites the transfer is from an octahedral site and in consequence may be weaker. It is therefore not a trivial matter to compare data from different structural types.

References

1 L. J. de Jongh and A. R. Meidema, *Adv. Phys.*, 1974, **23**, 1.
2 R. Rodríguez, A. Fernández, A. Isalgué, J. Rodriguez, A. Labarta, T. Tejada and X. Obradors, *J. Phys. C: Solid State Phys.*, 1985, **18**, L401.
3 P. D. Battle, T. C. Gibb, C. W. Jones and F. Studer, *J. Solid State Chem.*, 1989, **78**, 281.
4 T. C. Gibb, *J. Mater. Chem.*, 1992, **2**, 415.
5 P. D. Battle, T. C. Gibb, A. J. Herod, S.-H. Kim and P. H. Munns, *J. Mater. Chem.*, 1995, **5**, 865.
6 E. J. Cussen, J. F. Vente, P. D. Battle and T. C. Gibb, *J. Mater. Chem.*, 1997, **7**, 459.
7 M. P. Attfield, P. D. Battle, S. K. Bollen, T. C. Gibb and R. J. Whitehead, *J. Solid State Chem.*, 1992, **100**, 37.
8 T. C. Gibb and R. J. Whitehead, *J. Mater Chem.*, 1993, **3**, 591.
9 Y. Ishikawa, *J. Phys. Soc. Jpn.*, 1962, **17**, 1835–1877.
10 T. C. Gibb, A. J. Herod, S. J. Lees and P. D. Battle, *J. Mater. Chem.*, 1995, **5**, 285.
11 T. C. Gibb, *J. Mater. Chem.*, 1999, **9**, 2851.
12 U. Nowak and K. D. Usadel, *Phys. Rev. B*, 1989, **39**, 2516.
13 U. Nowak and K. D. Usadel, *Phys. Rev. B*, 1991, **43**, 851.
14 U. Nowak and K. D. Usadel, *Phys. Rev. B*, 1991, **44**, 7426.
15 U. Nowak and K. D. Usadel, *Phys. Rev. B*, 1992, **46**, 8329.
16 J. Esser, U. Nowak and K. D. Usadel, *Phys. Rev. B*, 1997, **55**, 5866.
17 M. Staats, U. Nowak and K. D. Usadel, *J. Magn. Magn. Mater.*, 1998, **177–181**, 85.
18 C. Pinettes and H. T. Diep, *J. Appl. Phys.*, 1998, **83**, 6317.
19 S. L. Ruby, B. J. Evans and S. S. Hafner, *Solid State Commun.*, 1968, **8**, 277.
20 V. A. Bokov, G. V. Novikov, Yu. G. Saksonov, V. A. Trukhtanov and S. I. Yuschuk, *Sov. Phys. JETP*, 1969, **29**, 403.
21 G. V. Novikov, V. A. Trukhtanov, L. Cser, S. I. Yuschuk and V. I. Goldanskii, *Sov. Phys. Solid State*, 1975, **16**, 2364.
22 B. J. Evans and L. J. Swartzendruber, *Phys. Rev. B*, 1972, **6**, 223.
23 F. Grandjean, G. J. Long, G. Longworth and B. J. Laundy, *Inorg. Chem.*, 1984, **23**, 1886.
24 T. C. Gibb, *J. Chem. Soc., Dalton Trans.*, 1983, 2035.